Journal of Structural Geology, Vol. 15, Nos 3–5, pp. 593 to 608, 1993
Printed in Great Britain

0191–8141/93 $06.00 + 0.00

Interference between pluton expansion and non-coaxial tectonic deformation: three-dimensional computer model and field implications

GIOVANNI GUGLIELMO, JR

Department of Geological Sciences, University of California, Santa Barbara, CA 93106, U.S.A.

(*Received* 13 *January* 1992; *accepted in revised form* 27 *July* 1992)

Abstract—Pluton emplacement contributes to the complexity of structures in orogenic belts because the geometry of these structures is often controlled by interactions between regional tectonic-related and local pluton-related strain fields. Many questions remain about the genesis of these structures. For example: (1) to what extent does pluton-related strain contribute to the formation of these structures? (2) what is the three-dimensional geometry of these structures? and (3) how does this geometry change with progressive deformation? The present simulation models in three dimensions the position, type and kinematic evolution of structures around plutons that expand in a non-coaxial tectonic environment.

The simulation generates patterns of four parameters: strain ellipsoid shapes and magnitudes, and orientation of foliation and mineral stretching lineations. Concave, lens-shaped, regions of high strain form on the sides of the pluton, whereas ellipsoidal regions of low strain form at the ends. In addition, foliation, stretching lineations, and constrictional regions form irregular three-dimensional rings around the pluton. Higher tectonic-related strains and strain rates favor rings that migrate towards the pluton, whereas higher expansion-related strains and strain rates favor ring migration away from the pluton. Furthermore, ring migration rates are much slower than tectonic deformation rates or expansion rates.

Although analyses of natural strain fields should always be carried out in conjunction with radiometric age determinations, structural and microstructural analysis and strain measurements, the simulated strain patterns offer practical guidelines for field work. Specifically, these patterns can be used to evaluate: (1) the origin, geometry and evolution of structures around plutons; (2) the three-dimensional sense of movement and orientations of ductile shear zones; and (3) the contribution of pluton-related strains to deformation of country rocks in orogenic belts.

INTRODUCTION

PLUTONS are commonly emplaced into crust that undergoes non-coaxial deformation (Nicolas *et al.* 1977, Berthé *et al.* 1979, Kerrich *et al.* 1980, Brun & Pons 1981, Hutton 1981, 1982, 1988, Lagarde & Choukroune 1982, Castro 1986, Guineberteau *et al.* 1987, Gapais 1989, Lagarde *et al.* 1990, Sacks & Horton 1991, Tikoff & Teyssier 1991). Some plutons permissibly fill zones of extension (Hutton 1982, 1988, Castro 1986, Guineberteau *et al.* 1987, Sacks & Horton 1991, Tikoff & Teyssier 1991), while others expand forcefully (Brun & Pons 1981, Holder 1981, Castro 1986, Ramsay 1989).

The interactions between local pluton expansion strain fields and regional tectonic-related strain fields largely control the orientation and distribution of structures observed in orogenic belts. The possibility that strain domains change in three dimensions as a result of tectonic deformation and pluton expansion was raised by Brun & Pons (1981) and Brun (1983). However, at present, little is known about the three-dimensional geometry of these strains and structures and how this geometry changes with progressive deformation.

Pluton emplacement kinematics have been studied using centrifuged models (Ramberg 1967, 1970, Ramberg & Sjöström 1973, Talbot, 1974, Soula, 1982, Talbot & Jackson 1987, Jackson & Talbot 1989) and studies of salt diapirs (Howard 1968, 1971, Sorgenfrei 1981, Woïdt 1978, O'Brien 1987, Talbot & Jackson 1987). However, in only a few models are the resulting strain patterns around plutons quantified (Dixon 1975, Schwerdtner & Troeng 1978, Morgan 1980, Brun & Pons 1981, Cruden 1988, Schmeling *et al.* 1988). In addition, only two studies used computer modeling to examine the structural patterns around plutons subjected to tectonic deformation (Brun & Pons 1981, Mandal & Chakraborty 1990), and these were both two-dimensional models.

This paper describes a kinematic three-dimensional simulation of expanding plutons in a non-coaxial tectonic environment. It simulates pre-, syn- and post-tectonic pluton emplacement and variations in local and tectonic strain rates. It suggests (1) how position, type and evolution of structures and strains change in three dimensions with progressive deformation; (2) how strain and structural patterns around plutons can be used to study three-dimensional sense of movement in, and orientations of ductile shear zones; and (3) that pluton-related strains contribute more than previously thought to deformation of country rocks in orogenic belts.

PLUTON-RELATED STRAINS IN OROGENIC BELTS

Deformation resulting from pluton expansion in a tectonic environment is complex. For example, several combinations of pluton-related and tectonic-related strain rates are possible. Therefore, it is difficult to determine: (1) whether pluton- or tectonic-related deformation changed a given parameter of the strain ellipsoid; and (2) which deformation path each strain

parameter follows during progressive deformation. In addition, pluton-related and tectonic-related strain rates may selectively alter some strain parameters while other parameters remain unchanged. For example, pluton expansion may alter the distribution of strain ellipsoid shapes and intensities, but not change significantly the orientation and distribution of extension axes (stretching lineations) or flattening planes (foliations). Consequently, during field work, it is difficult to distinguish trivial structures and structural patterns from the ones that constrain pluton-related and tectonic-related kinematics.

Complexity of natural strain paths increases because strain rates may vary during progressive deformation. In addition, a pluton may be emplaced before, during or after tectonic deformation. All these possible strain paths can produce a large number of strain patterns in the country rock. The number of possible patterns is further increased because the interaction between pluton-related and tectonic-related strain fields creates strain patterns in three dimensions. Each of the possible slices of a particular three-dimensional pluton produces distinct two-dimensional patterns in map view.

These orogenic belt complexities cannot be reproduced numerically without integration of several computer-simulation techniques such as interactive modeling, multiple-window viewing and three-dimensional representations.

MODEL DESCRIPTION

Interactive simulation allows us to change values of strain tensors and strain rates during the simulation. In addition, interactivity allows us to monitor how strain patterns change during progressive deformation in real-time. This instantaneous monitoring helps eliminate hundreds of redundant strain patterns rapidly, with the confidence that no essential pattern is discarded. Multiple-window viewing was instrumental in the analysis of four strain-ellipsoid parameters at the same time. The computer screen displays changes in strain-ellipsoid shapes and intensities as well as orientations of stretching lineations and foliations simultaneously. This integrated analysis made it possible to determine how pluton-related and tectonic-related strain paths affected each of these parameters of the strain ellipsoid. Finally, three-dimensional rendering (Figs. 1 and 2) allowed the visualization of the three-dimensional strain patterns and, by slicing these, the determination of map patterns. Computer graphics and programming aspects of the simulation are described by Guglielmo (1992).

The simulation assumes that a spherical pluton expands radially, and produces strain gradients in the country rock. These gradients were modeled kinematically based on natural plutons and published models. Strain patterns next to concordant natural plutons were based on field measurements around the Ardara (Sanderson & Meneilly 1981) and Merrimac plutons (Guglielmo 1993). Around these plutons, and in the simulation, flattening strain ellipsoids are oriented concentrically and strain intensities gradually decrease away from the pluton. Strain gradients far from the pluton were simulated based on physical and computer models (Dixon 1975, Cruden 1988, Schmeling *et al.* 1988), which show that, in a ductile crust, pluton-related strains decrease gradually away from the pluton and may reach distances of a few body radii from the pluton. In addition, integration of field and three-dimensional computer models shows that pluton-related strains may affect country rock at least as far as half a body radius from the pluton (see below).

Fig. 1. (a)–(d) Two-dimensional strain and structural patterns around a pluton that expands during regional simple shear. Four parameters analyzed simultaneously constrain the sense of shear and pluton expansion kinematics (see text). (a) Left: undeformed simulation grid. Right: strain magnitude. The regional shear plane is parallel to the *XZ* co-ordinate plane and the arrow gives the sense of shear. Dark blue represents areas of low strain magnitude. (b) Foliation defined by traces of *XY* planes of the strain ellipsoid. Note the foliation triple points at the ends of the pluton. (c) Strain ellipsoid shape contoured in values of Lode's parameter. 'Blue' represents constriction and 'pink' represents flattening. (d) Stretching lineations defined by the major axis of the strain ellipsoid. Note that the *XY* co-ordinate plane is approximately horizontal (rather than parallel to the page as in a–c) which helps clarify the orientation of lineations. Also, note that vertical mineral stretching lineations at the ends of the pluton occupy an area larger than the area of constrictional strains shown in (c). Patterns (a)–(d) are cross-sections through the center of three-dimensional models in (j) and Figs. 2(a) & (b). (e)–(h) Same as (a)–(d), respectively, but at a more advanced stage of deformation. Tectonic deformation rates are higher than expansion rates. (e) Blue low-strain zones form at the ends of the pluton. Foliation triple points (f), constrictional regions (g), and areas of vertical stretching lineations (h) move towards the pluton. The tectonic displacement rate is higher than the rate of migration of the constrictional points, as shown by the tectonic displacement vector (arrow) being larger than the change in distance between the triple point and the pluton (cf. c and g). Patterns (e) and (g) are cross-sections through the center of pluton in (i) and (l), respectively. (i) Three-dimensional strain magnitudes. The yellow elongate ellipsoid (I) in the center represents the pluton, and arrows show the sense of shear and the *XZ* shear plane. Pink lens-shaped zones of high strain form on the sides (II) of the pluton, whereas ellipsoidal low-strain zones form at the ends (III) of the pluton. A cross-section subparallel to the paper and through the center of the three-dimensional pluton produces the two-dimensional slice shown in (e). Surface (II) corresponds to the boundary between the green and yellow areas in the slice; therefore strain magnitudes in the high-strain regions range between 1.5 and 2. Conversely, surface (III) corresponds approximately to the dark blue low-strain zones, where strains are lower than 0.5. This example illustrates how three-dimensional surfaces control map and cross-section patterns. (j) Three-dimensional Lode's parameter. The green ball (I) in the center of the picture represents the pluton. The three-dimensional arrows illustrate the regional shear. The green irregular surface (II) is the locus of points of plane strain separating regions of constrictional from regions of flattening. Flattening is dominant in the illuminated region (III) on top of the pluton and in the dark region (IV) at the bottom of the pluton. Conversely, constriction forms an irregular ring that is narrow at the ends (little arrow) and wide at the sides (V) of the pluton. Pink surfaces (VI) envelop the highest constrictional strains and the best-developed mineral stretching lineations in the region. Surface (II) corresponds to the boundary between the green and the yellow areas in (c), and surface VI corresponds to the boundary between the blue and green areas. (k) Same as (j), but to provide a rotated view from the top. Notice the constrictional ring far from the pluton (little arrow). (l) Similar to (k) but at a more advanced stage of deformation. This corresponds to the two-dimensional slice shown in (g). Note that the constrictional ring approaches the pluton with progressive deformation.

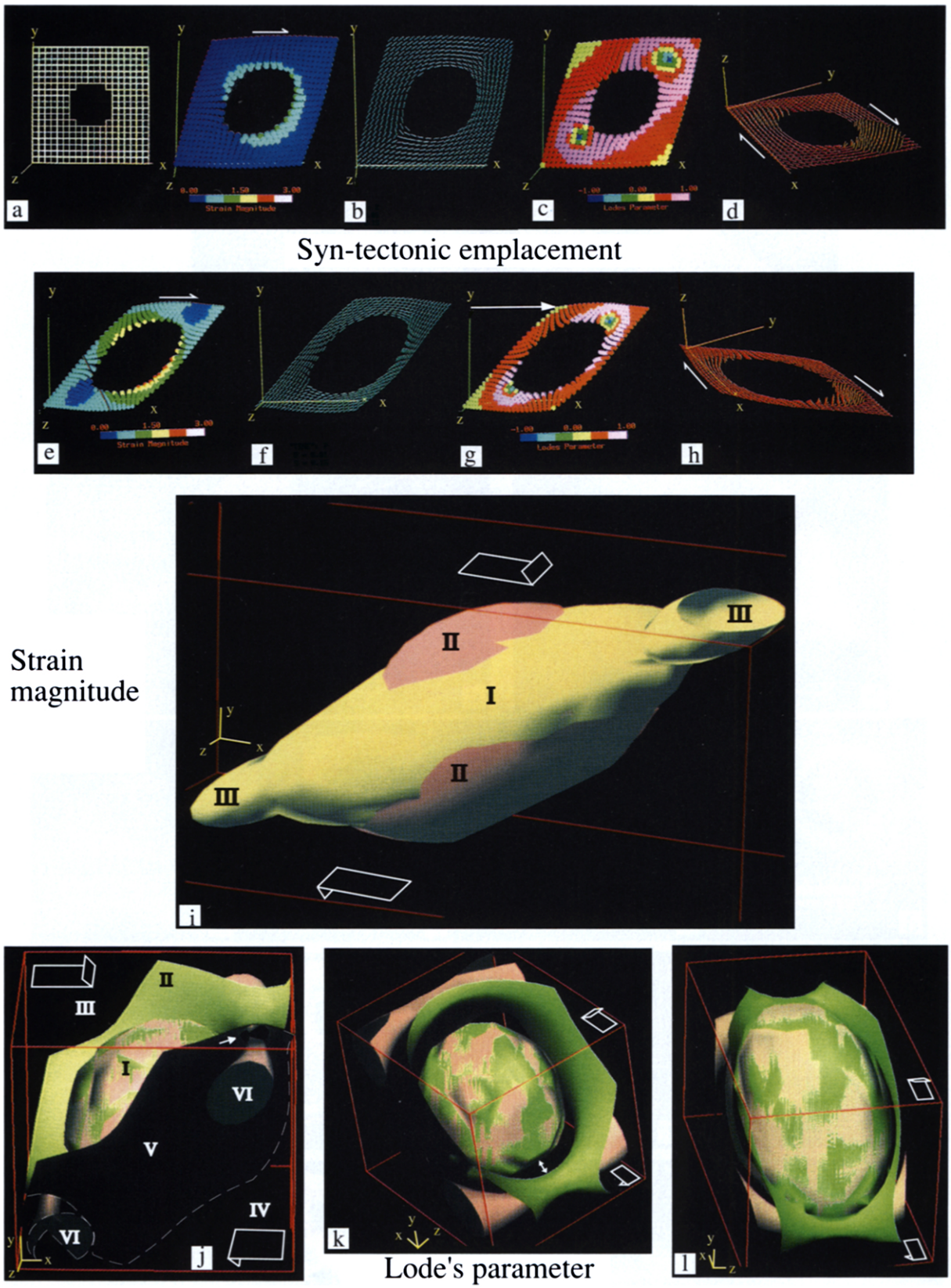
a
b
c
d
Syn-tectonic emplacement
e
f
g
h
Strain magnitude
i
II
III
I
II
III
j
II
III
I
VI
V
IV
VI
k
l
Lode's parameter

Fig. 1.

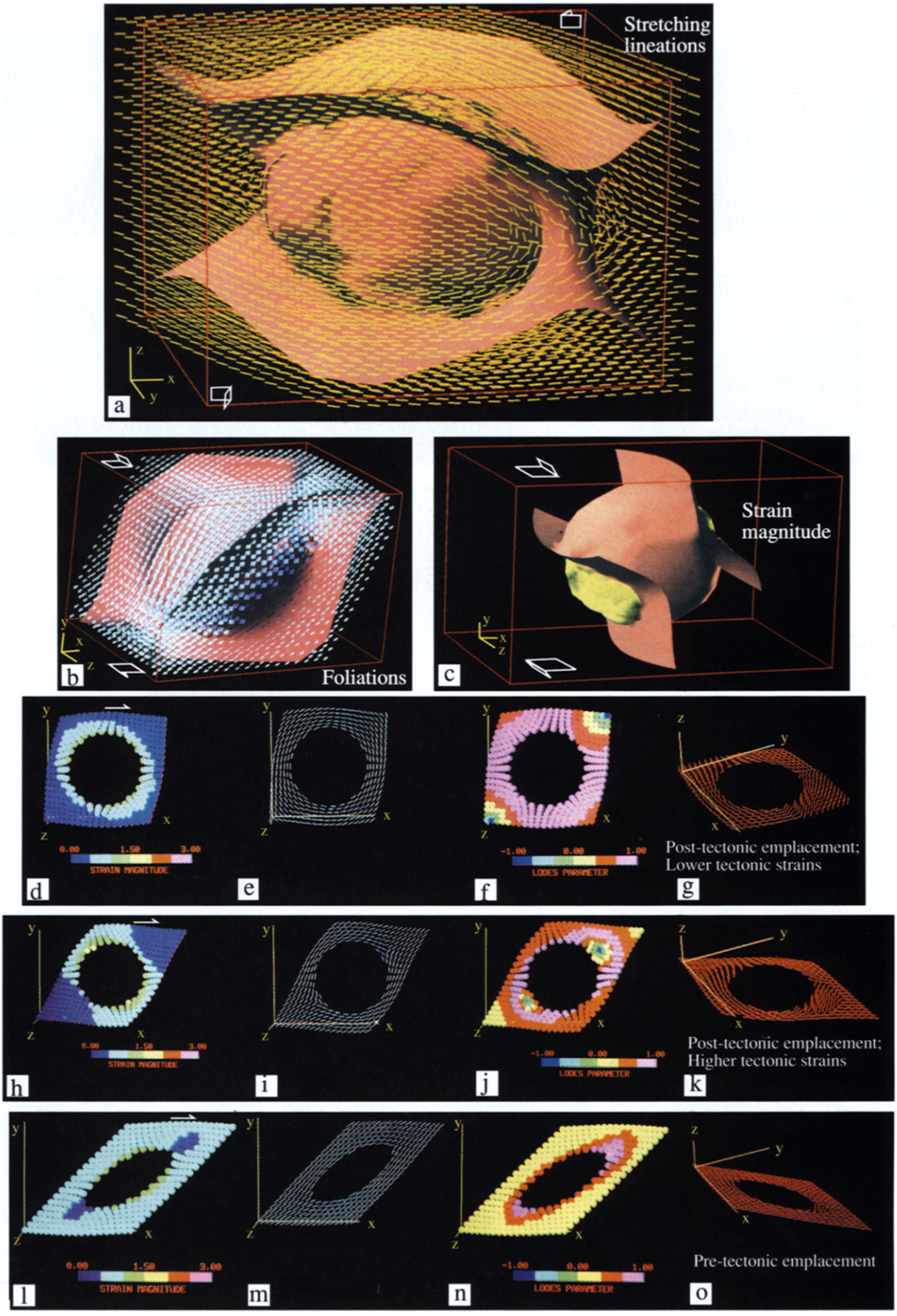
Stretching lineations
a
b
Foliations
c
Strain magnitude
d
e
f
g
Post-tectonic emplacement;
Lower tectonic strains
h
i
j
k
Post-tectonic emplacement;
Higher tectonic strains
l
m
n
o
Pre-tectonic emplacement

Fig. 2.

The pluton may be emplaced before, during or after regional deformation, which is modeled as being homogeneous, ductile and dominated by simple shear. The simulation grid is deformed using smooth functions (see the Appendix) so strains across boundaries between grid elements remain compatible during progressive deformation. As in any modeling, modeled patterns are consistent with the kinematic schemes that created them. However, other kinematic schemes may produce similar patterns (Guglielmo 1990, in press a).

STRAIN PATTERNS

During syn-tectonic pluton expansion in a non-coaxial tectonic environment the pluton becomes an ellipsoid whose major axis is oblique to the direction of regional shear. Throughout this paper the word '*ends*' of the pluton refers to regions in the country rock near the pluton where the contact between pluton and wall rock has the sharpest curvature. Conversely, '*sides*' of the pluton refers to wall rock near the contact that has the lowest curvature. '*Top*' of the pluton is defined assuming strike-slip shear. That is, the main regional simple-shear plane is vertical, and regional particle displacement lines are horizontal and parallel to this simple-shear plane (Fig. 3a).

During pluton expansion in a non-coaxial tectonic environment, interference between pluton-related and tectonic-related strain fields at the 'ends' of the pluton is distinct from interference at the 'sides' of the pluton. The geometry of these interferences controls the intensity, type and geometry of structures found around plutons. The three-dimensional geometry of these structures and how this geometry changes during progressive deformation has not been previously described.

Strain magnitude

Strain magnitude (Nadai 1963) is given by:

$$\bar{\varepsilon}_s = \frac{1}{\sqrt{3}}[(\varepsilon_1 - \varepsilon_2)^2 + (\varepsilon_2 - \varepsilon_3)^2 + (\varepsilon_3 - \varepsilon_1)^2]^{1/2},$$

where ε_1, ε_2 and ε_3 are principal logarithmic strains given by

$$\varepsilon_1 = \ln(1 + e_1); \qquad \varepsilon_2 = \ln(1 + e_2)$$

and

$$\varepsilon_3 = \ln(1 + e_3)$$

and $(1 + e_1)$, $(1 + e_2)$ and $(1 + e_3)$ are the lengths of the strain ellipsoid semi-axes. e_1, e_2 and e_3 are the values of the principal strains.

Patterns of strain magnitude are worth modeling because they control the *intensity* of fabrics around the pluton. In regions of high strains, foliations and lineations are usually more conspicuous and easier to measure than in regions of low strain. In addition, high strains favor the resetting of quartz fabrics and other microstructures. Conversely, in low-strain zones, fabrics are less developed. Nevertheless, in low-strain zones, fabrics formed during previous deformation events may be better preserved during subsequent deformation.

Furthermore, strain magnitudes around plutons affect the quantity, orientation and structural history of hydrothermal veins. Regions of high strains are characterized by dissolution of country rock minerals. The resulting fluids, in conjunction with fluids from the pluton, produce hydrothermal solutions that precipitate in low-strain zones. In addition, in regions of high strains, veins and dikes tend to rotate towards parallelism with the pluton contact. In low-strain zones, veins are more likely to preserve their primary structures and orientation, and multiple generations of cross-cutting veins may be distinguished.

The distribution of strain magnitude around plutons may affect the geometry of the contact between pluton and wall rock. In areas of high strains, contacts that were originally discordant due to interfingering between pluton and wall rock may rotate to become smooth and concordant with wall-rock foliation. Conversely, in low-strain zones, the geometry of the original contact may be preserved.

In summary, the intensity, geometry and chances of preservation of structures during progressive deformation around a pluton strongly depend on whether these structures are located in regions of high or low strain.

Modeled strain magnitude patterns

During pluton expansion in a non-coaxial tectonic environment, low-strain zones (small yellow areas at the

Fig. 2. (a) Three-dimensional pattern of mineral stretching lineations. The pink surfaces show the pluton and the constrictional ring. This is a rotated version of Figs. 1(j) or (k) and represents a pluton emplaced along a *strike-slip* shear zone. Arrows indicate the vertical shear plane subparallel to the paper. Yellow lines of constant length show the orientation and distribution of mineral stretching lineations. Without real-time three-dimensional rotations seen on a computer screen, it is difficult to see whether the lineations plunge towards or away from the viewer. Therefore, the main lineation domains are simplified in Fig. 3(a). (b) Three-dimensional pattern of foliations. The pink surface is one of plane-strain and it shows the constrictional ring (as in Fig. 1j) around the pluton. The blue squares represent orientations and distribution of foliation planes. Again, visualization of the trends of the foliation planes is difficult without real-time rotations of the model. Therefore, the main foliation domains are simplified in Fig. 3(a). (c) A post-tectonic pluton in three dimensions. The spheroid in the center represents a pluton that expanded after regional deformation. The pink surfaces correspond to the boundaries between the dark blue and light blue areas in the two-dimensional slice shown in (h). (d)–(g) Strain and structural patterns (see explanations in the caption to Figs. 1a–d) formed during post-tectonic pluton expansion. Notice the subspherical shape of the pluton. Patterns in the wall rock are similar to those formed during syn-tectonic expansion. (h)–(k) The same post-tectonic expansion as in (d)–(g), respectively, however here the pluton is emplaced in a crust that has undergone a greater regional tectonic strain. Notice that the constrictional rings are closer to the pluton (cf. f & j). (l)–(o) Patterns produced by pre-tectonic pluton expansion (see explanations in caption to Figs. 1a–d).

ends of the pluton in Fig. 1i) have the shape of an ellipsoid whose major axis is approximately parallel to the major axis of the pluton. Conversely, regions of high strain assume a three-dimensional convex lens shape (pink 'bowls' at the sides of the pluton in Fig. 1i).

Absolute values of strain magnitude are shown in a two-dimensional slice (Fig. 1e) through the center of the three-dimensional pluton and subparallel to the plane of the paper (Fig. 1i). Within the three-dimensional low-strain zone (Fig. 1i), strain magnitudes are lower than 0.5 and correspond approximately to the dark blue area in the two-dimensional slice. On the other hand, within the high-strain three-dimensional regions, strain magnitudes are higher than 1.5 and correspond to the yellow area in the slice.

During progressive deformation, patterns of strain magnitude at the sides of the pluton are different from the patterns at the ends of the pluton. At the sides of the pluton, pluton-related and tectonic-related displacement vectors form low angles. Consequently, regional- and pluton-related strain fields add up to faster total strain rates, which, in turn, produce high total strains at any stage of the deformation. Conversely, at the ends of the pluton, the angle between pluton-related and tectonic-related displacement vectors is high (close to 90°). Consequently, regional- and pluton-related strain fields interfere and partially cancel each other out, slowing down total strain rates. As a result, total strain intensities at the ends of the pluton are lower than on the sides of the pluton during the whole deformation history. At late stages of deformation these low-strain zones become slightly asymmetrical to the long axis of the pluton (e.g. Figs. 1e & i).

During progressive deformation, the relative rate of pluton expansion with respect to rate of tectonic deformation has subtle effects on pluton shape, strain magnitude patterns and strain magnitude path. Higher expansion rate with respect to tectonic deformation rate: (1) makes the pluton more equidimensional; (2) increases strain magnitudes at the sides of the pluton; (3) delays formation of low-strain zones; and (4) favors low-strain zones that are larger and asymmetrical with respect to the major axis of the pluton.

Conversely, higher tectonic deformation rate with respect to expansion rate makes the pluton more elongate and enhances the formation of well-defined, small and symmetrical low-strain zones early in the deformation history.

Strain shape

The 'degree of flatness' or shape of the strain ellipsoid can be expressed by Lode's parameter (Lode 1926):

$$\nu = \frac{2\varepsilon_2 - \varepsilon_1 - \varepsilon_3}{\varepsilon_1 - \varepsilon_3}.$$

Lode's parameter can assume values between -1 and 1, with negative values representing constriction and positive values representing flattening. $\nu = 0$ represents plane strain.

Patterns of strain shape control the *types* of structures around the pluton. In regions of high constriction, mineral stretching lineations are more conspicuous and easier to measure than in regions of low constriction, therefore L tectonites predominate over S tectonites. Conversely, in regions of high flattening, S tectonites predominate over L tectonites.

Modeled strain shape patterns

During pluton expansion in a non-coaxial environment, a three-dimensional, irregular, surface separates areas of constriction from areas of flattening (Figs. 1j & k). Regions of constriction are wide on the top and bottom of the pluton, and form narrow vertical tubes at the ends of the pluton. Conversely, regions of flattening are on the sides of the pluton, and at the ends of the pluton beyond the region of constriction.

Absolute values of Lode's parameter are shown in a two-dimensional slice (Fig. 1c) through the three-dimensional pluton (Fig. 1j). The slice, cut through the center of the pluton, is parallel to the plane of the paper. The green surface (Fig. 1j) is the locus where Lode's parameter equals zero and it corresponds to the boundary between the green and yellow areas in the two-dimensional slice. Within the region between the pluton and the green surface (Fig. 1j), Lode's parameter is between 0 and 1. This region corresponds to the yellow, red, and pink areas in the two-dimensional slice. Finally, on the sides of the pluton (dark region on Fig. 1j) values of Lode's parameter are between 0 and -1, and this corresponds to the green and blue areas in the two-

Fig. 3. (a) Foliation and stretching lineations form irregular rings around the pluton. Syn-tectonic simple shear (arrows) and pluton expansion transformed an initial parallelepiped (white dashed lines) into a prism (black lines). The background photograph is the same as Fig. 2(a), in which the irregular surface around the pluton separates regions of constriction from regions of flattening. Shaded planes represent average orientations of foliation, and thick white dashes represent average orientations of lineations. Foliations form a ring with an equilateral triangular section at the ends of the pluton (I), and an isosceles triangular section at the top of the pluton (II). Foliations are parallel to the pluton next to the pluton (III) and parallel to regional strains away from the pluton (IV and VI). Stretching lineations at the ends of the pluton near the ring (V and IV) are orthogonal to lineations within the ring (I). Near the ring at the ends of the pluton, lineations are vertical close to the pluton (V) and horizontal far from the pluton (IV). Lineations are horizontal at the sides (III) and top (VI) of the pluton. (b) Different erosional planes have distinct strain shape and stretching lineation map patterns. Background photograph is the same as in (a). Erosional plane (I) cuts the center of the pluton and displays vertical lineations and constrictional points in the map view. Erosional plane (II) displays plunging lineations and crescentic areas of constriction. Erosional plane (III) displays horizontal stretching lineations and constriction all around the pluton. Erosional planes oblique to planes (I), (II) and (III) may display asymmetrical two-dimensional patterns. (c) The orientation of erosional planes (I–VII) with respect to the regional displacement field (arrows) controls the map patterns of strain magnitude and the type of shear zone produced. For example (I) and (VII) correspond to a strike-slip shear zone; (III) and (V) to a reverse shear zone, and (II), (IV) and (VI) to a normal shear zone. Shear zones of these different types produce distinct strain magnitude patterns, shown in Fig. 4.

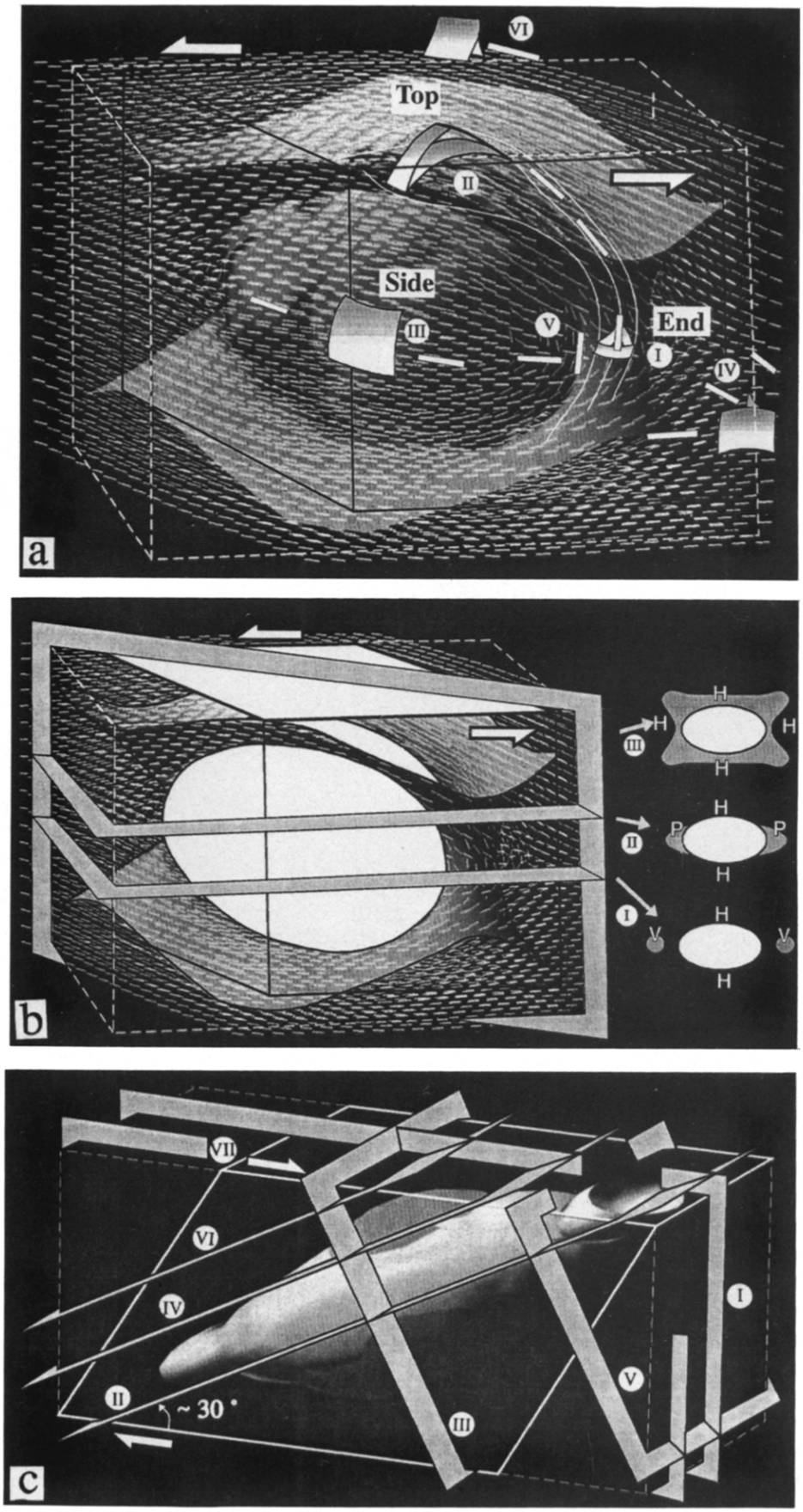
VI
Top
II
Side
III
V
End
I
IV
a
H
H
H
H
III
P
P
II
I
V
V
b
VII
VI
IV
II
~ 30 °
III
V
I
c

Fig. 3.

dimensional slice. The highest constrictional strains in the area are located within the pink surfaces (Figs. 1j or 1k). These surfaces correspond to the blue constrictional points in the two-dimensional slice. Notice that regions of high constrictional strains may be discontinuous in three dimensions (little arrow in Fig. 1j).

During progressive syn-tectonic deformation, constrictional rings migrate (cf. Figs. 1k & l). Real-time simulation was specially useful in showing that rates of ring migration are much slower than rates of tectonic deformation or pluton expansion. Comparison of initial and final strain patterns also documents the slow ring migration rates. For example, distances between ring and pluton changed little compared with the displacements caused by tectonic deformation (cf. Figs. 1c and g).

During progressive deformation, the relative rate of pluton expansion with respect to the rate of tectonic deformation affects the size and position of constrictional regions. Higher expansion rates with respect to tectonic deformation rates increase the size of constrictional regions and push them away from the pluton. Conversely, higher tectonic rates with respect to expansion rates make regions of constriction smaller, more elongate and closer to the pluton.

Foliation and stretching lineations

Foliations (cleavage and schistosity) and mineral stretching lineations are worth modeling because these are commonly the most conspicuous fabric in the country rock and are used to infer critical field relationships. For example, these structures produce strong anisotropies that control subsequent (1) brittle or ductile deformation, (2) fluid migration and (3) orientation and shape of dikes and sills. In addition, overprinting relationships of foliation and stretching lineations are used to establish sequences of deformational events. Furthermore, bedding–cleavage relations are used to determine right-way-up directions in highly deformed terrains.

In addition, foliations and stretching lineations give quick information about parameters of the strain ellipsoid (Ramsay & Huber 1983). These structures give indirect and qualitative characterizations of strain patterns that are easy to obtain and can, in part, compensate statistically for the inaccuracy or lack of quantitative strain measurements. Foliation usually forms parallel to the XY plane of the strain ellipsoid, whereas lineation forms parallel to the X axis of the strain ellipsoid. Therefore, these structures give good constraints on strain ellipsoid *orientation* and *distribution*. Descriptions of how well developed foliations and lineations are in a given rock type can aid in separating zones of high strain *magnitude* from zones of low strain. Finally, field distinction among L, S and L–S tectonites may produce a rough map that qualitatively separates areas of *constriction* from areas of *flattening*. In the absence of true strain markers, these qualitative observations of planar and linear fabrics may be used to construct field maps of strain patterns that, subsequently, can be compared with modeled patterns in order to constrain shear zone kinematics and the contribution of pluton-related strains to the deformation of the country rock (see below).

Modeled foliation patterns

In rocks subjected to non-coaxial deformation, foliation patterns around an expanding pluton are complex. At the top and ends of the pluton, foliation forms a three-dimensional irregular ring around the pluton, and is located approximately within the three-dimensional region of constriction (Figs. 1b, 2b and 3a). The ring has a triangular cross-section, consistent with two-dimensional patterns modeled by Brun & Pons (1981). However, in three dimensions, this section is large and isosceles on the top of the pluton, and small and equilateral at the ends of the pluton. On top of the pluton the orientation of foliation changes with distance from the pluton; specifically, foliation is parallel to the pluton contact next to the pluton, and is parallel to regional strains away from the pluton (Fig. 3a).

The amounts of total tectonic strain and total expansion strain displace the foliation ring. Higher total tectonic strain brings the ring closer to the pluton and higher expansion strain displaces the ring away from the pluton. This motion is consistent with the displacements of two-dimensional triple points described by Brun & Pons (1981).

Furthermore, the rate of pluton expansion with respect to the rate of tectonic deformation affects the position of the foliation ring. During progressive deformation, higher expansion rates with respect to tectonic deformation rates displace the ring away from the pluton. Conversely, higher tectonic deformation rates with respect to expansion rates bring the ring closer to the pluton. Rates of ring migration are much slower than the rates of tectonic deformation or rates of pluton expansion.

Modeled lineation patterns

The top and ends of the pluton show lineations aligned along an irregular three-dimensional ring around the pluton (Figs. 2a and 3a). This ring: (1) approximately follows the orientation of the three-dimensional region of constriction; (2) is larger than this region; and (3) has a half-moon-shaped two-dimensional orthogonal section (Figs. 1d & h and 2a). The two-dimensional section is large and flat on top of the pluton. Conversely, this section is smaller and more equi-dimensional at the ends of the pluton (Figs. 1d & h and 2a). Consequently, lineations at the ends of the pluton form high angles with lineations on the sides of the pluton in three dimensions (Figs. 2a and 3a).

Lineation patterns on the sides of the pluton contrast with patterns at the top and ends. On the sides and next to the pluton lineation is: (1) parallel to the pluton contact; (2) parallel to the elongation of the pluton; and (3) concordant with lineations on the top of the pluton. Conversely, on the sides and away from the pluton

lineations are parallel to regional particle displacement paths (Figs. 1d & h, 2a and 3a).

During progressive deformation, the volume of the lineation ring diminishes (cf. Figs. 1d & h). The rate of change in volume of the lineation ring is much slower than the rate of tectonic deformation or rate of pluton expansion. During progressive deformation, relative rates of pluton expansion with respect to rates of tectonic deformation affect the position of the lineation ring. Higher expansion rates with respect to tectonic deformation rates push the ring away from the pluton. Conversely, higher tectonic deformation rates with respect to expansion rates bring the ring closer to the pluton.

Pre- and post-tectonic cases

During post-tectonic intrusion, the pluton expands after regional simple shear and remains equidimensional (Figs. 2c–k). Conversely, during pre-tectonic emplacement, the pluton becomes more elongate than during syn-tectonic deformation (Figs. 2l–o).

Post- and pre-tectonic pluton expansion are examples of how different strain paths can produce similar final structures. Unlike the syn-tectonic situation, during post-tectonic pluton expansion strain patterns depend on the amount of tectonic strain in the country rock before pluton emplacement, and on the amount of post-tectonic expansion. However, the resulting patterns are analogous to patterns produced during syn-tectonic emplacement. Higher expansion-related strains (Figs. 2d–g) favor a pattern of: (1) high strain intensities uniformly distributed around the pluton (Fig. 2d); (2) large constrictional areas (Fig. 2f); and (3) constrictional, foliation, and lineation rings away from the pluton (Figs. 2e–g). Conversely, higher total tectonic strains before expansion (Figs. 2h–k) favor a pattern of: (1) well-defined low-strain zones (Figs. 2c & h); (2) small constrictional regions (Fig. 2j); and (3) constrictional, foliation, and lineation rings closer to the pluton (Figs. 2i–k).

During pre-tectonic expansion, strain paths are different again from syn- and post-tectonic cases. During the pre-tectonic case, the pluton expands first and then is tectonically deformed, however, the strain magnitude patterns are similar to the ones around syn- and post-tectonically emplaced plutons (Figs. 2l–o).

FIELD IMPLICATIONS

In addition to revealing the three-dimensional geometry of structures formed around plutons during pluton expansion and non-coaxial tectonic deformation, the modeled patterns shed light on the following unanswered questions. (1) How do three-dimensional rings and their evolution control the structures at the ends of expanding plutons? (2) Why are documented rings (or triple points in map view) comparatively rare? Is triple point rarity due to lack of detailed structural mapping? Or are the formation, evolution and exposure of rings not conducive to their preservation in the geological record? (3) How far from expanding plutons does pluton-related deformation affect the country rock?

Strain migration and superposition of structures

The complexity of structures and microstructures at the ends of plutons depends on the direction and rate of constrictional ring migration. For any fixed point around a natural pluton, progressive deformation causes changes in the shape, orientation, intensity and position of the strain ellipsoid. Changes in strain *intensity*, by themselves, produce a relatively simple strain path. However, changes in ellipsoid *orientation* and *shape* may cause superposed structures and fabrics that may record complex strain paths in outcrop.

The sides and ends of the pluton record distinct strain paths in the models. Therefore, these regions are expected to contain distinct fabrics and textures in the field. At the sides of the pluton, modeled ellipsoid *shapes* and *orientations* remain approximately constant during deformation. Therefore, although strain *intensity* increases, superposition of fabrics and structures is expected to be relatively simple, except where, locally, regions of shortening may become regions of extension during progressive flattening of the strain ellipsoid (Ramsay & Huber 1983). On the other hand, at the top and ends of the pluton, ring migration causes complex regional superposition of fabrics and structures in the field. Migration of constrictional rings into a region of flattening may produce a strain interference trail where: (1) vertical lineations partially transpose horizontal lineations; (2) foliation in newly formed triangles crenulates earlier foliations; (3) inclusion trails in contact metamorphic porphyroblasts record multiple deformations; and (4) constrictional ellipsoids are superposed on flattening ellipsoids. Either regions of shortening are superposed upon regions of extension producing, for example, folded boudins; or extension is superposed upon shortening producing, for example, boudinaged folds.

In summary, these simulations suggest the constrictional ring migrates towards the pluton with increasing tectonic deformation rates, and away from the pluton with increasing expansion rates. The direction of ring migration controls: (1) the area affected by strain-ellipsoid interference trails; and (2) whether flattening will be superposed upon constriction or vice versa.

Preservation of superposed structures

Predicted rates of ring migration do not favor preservation of interference trails in the geological record. The simulations show that rates of ring migration are much slower than rates of tectonic deformation or pluton expansion. If the country rock deforms smoothly, slower

rates of ring migration may provide time for re-equilibration of previous fabrics to new strain regimes formed during ring migration. This re-equilibration tends to eliminate trails from the geological record. In addition, the ring and ring trails form next to the pluton, where pluton-related high temperatures and percolation of fluids enhance re-equilibration of ring structures and shorten strain memory. These pluton-driven effects further degrade trails.

Preservation of constrictional strain rings

Whereas preservation of a disturbed strain interference trail is uncertain, preservation of the last-formed strain ring is likely. Preservation of the ring and its structures will depend on rates and paths of deformation. At first sight, constrictional ring preservation seems unlikely because rings may migrate towards and disappear into the pluton with progressive tectonic deformation. However, rates of ring migration are significantly slower than rates of pluton- or tectonic-related deformation. Slower migration rates may allow constrictional rings to remain outside the pluton and to be preserved.

In addition, modeled patterns show that, if the country rock remains ductile, little change occurs in the orientation and position of the constrictional ring during pre-, syn- and post-tectonic pluton emplacement. Therefore, strain rings may persist long after pluton expansion is resumed. For example, let us assume that the emplacement history for a pluton follows three stages: (1) a wide shear zone, with a vertical shear plane, accumulates strain slowly for a long time (e.g. 10 Ma); (2) the shear zone is intruded by a pluton that expands quickly; and (3) after expansion stops due to fast (e.g. 1 Ma) crystallization of the pluton, tectonic deformation continues for a long period (another 10 Ma). For this scenario, modeled strain patterns suggest that, during step (1) plane strains and horizontal stretching lineations would form in the country rock. The pluton expands *after* this regional deformation, step (2). Consequently, interactions between local and regional strains produce constrictional rings in a *post-tectonic* expansion situation (Figs. 2d–k). These rings and related structures are enhanced during the short period of *syn-tectonic* expansion (Figs. 1a–h). Finally, during step (3) expansion has stopped and regional deformation continues. In other words, expansion happened *before* the current regional deformation. Therefore, ring formation is enhanced further, but now, in a *pre-tectonic* expansion situation (Figs. 2l–o). Consequently, the ring may be preserved throughout the deformation history.

In summary, modeled patterns suggest that (1) the presence of a strain ring is more dependent on total strains than on the sequence in which these strains are accumulated; and (2) strain rings are persistent during pre-, syn- and post-tectonic progressive deformation. This persistence increases the chances of strain rings becoming a part of the geological record.

Geological map patterns

The appearance of preserved constrictional rings and their structures in map view depends on the orientation of the erosional surface with respect to the constrictional ring. For example: if an erosional plane cuts the pluton near its center and is perpendicular to the constrictional ring, at the ends of the pluton (Fig. 3b, plane I) we should expect: (1) two equilateral foliation triangles; (2) two equidimensional areas of constrictional strains; and (3) vertical mineral stretching lineations.

If, on the other hand, the erosional plane passes near the top of the pluton (Fig. 3b, plane II), at the ends of the pluton we should expect: (1) two isosceles foliation triangles; (2) half-moon-shaped areas of constrictional strains; and (3) shallowly plunging mineral stretching lineations. Finally, if the erosional plane is parallel to the constrictional ring (Fig.3b, plane III), geological maps are expected to show: (1) no foliation triangles, and (2) constrictional strains and horizontal mineral stretching lineations all around the pluton.

These three examples illustrate how the three-dimensional modeled patterns aid the interpretation of structures and strains around plutons in map view.

Shear zone kinematics

Map-view strain patterns around plutons provide additional ways to constrain the three-dimensional kinematics in shear zones. The orientation of the erosional plane with respect to particle displacement paths in a regional shear zone controls whether a geological map will show a strike-slip, normal or reverse shear zone. However, the erosional plane orientation also controls strain patterns in map view. Therefore, two-dimensional patterns of strain and structures around plutons may be used to constrain the regional shear-zone orientation and sense of movement.

For example: the map patterns of strain magnitude will depend on the orientation of the shear zone with respect to the erosional plane. In strike-slip shear zones, erosional planes are approximately perpendicular to the shear plane and parallel to the particle displacement paths. For an erosional plane that cuts the center of the pluton, strain magnitude patterns in map-view for this shear zone show low-strain zones at the ends of the pluton and zones of high strain on the sides of the pluton (cf. Fig. 3c, plane I, and Fig. 4, plane I).

Conversely, in normal shear zones (e.g. Fig. 3c, planes II, IV and VI), the erosional plane makes an acute angle with the shear plane. In this example, let us assume the erosional plane cuts the pluton above its center (Fig. 3c, plane IV). There are no low-strain zones and high-strain zones at the ends of the pluton in map-view (Fig. 4, plane IV).

Analysis analogous to that described above, when done for all four modeled parameters in combination (strain magnitude, strain shape, foliations and stretching lineations), can provide good guidelines for studying shear-zone kinematics.

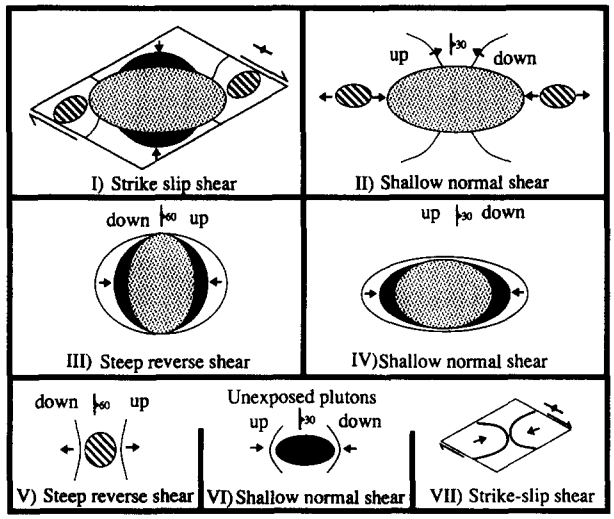

Fig. 4. Erosional planes of various orientations with respect to regional deformation produce distinct map patterns of strain magnitude. Patterns (I)–(VII) were produced, respectively, by planes (I)–(VII) from Fig. 3(c). Strike and dip symbols indicate the orientation of the regional shear plane. Stippled areas correspond to the pluton; black represents areas of high strain; stripes correspond to areas of low-strain; thin lines represent intermediate values of strain magnitude. Short, black arrows indicate maximum strain gradients, with head of arrow indicating higher strains. Examples of end-member map patterns of strain magnitude are: (I) strike-slip shear—high strains on the sides of the pluton have maximum strain gradients perpendicular to the pluton, and the low-strain zones at the ends of the pluton are asymmetrical; (II) normal shear zone—maximum strain gradients at the sides of the pluton are parallel to the pluton, and low-strain zones are symmetrical; (III) reverse shear zone—higher strains occur on the sides of the pluton, and low-strain zones are absent; (IV) normal shear zone—higher strains occur at the ends of the pluton; (V)–(VII) are patterns above unexposed plutons. Patterns (I)–(VII) can be used in combination with (1) field and microstructural patterns and (2) map-view patterns of Lode's parameter, foliations and stretching lineations derived from, for example, Figs. 3(a) & (b), in studying the three-dimensional nature of regional shear zones.

Background strains

Plutons unroofed by erosion may be responsible for the strain patterns in a geological map of the country rocks. Plutons below the erosional surface (e.g. Fig. 3c, planes V, VI and VII) may change strain gradients and patterns in the country rock (e.g. Fig. 4, planes V, VI and VII). These strain patterns may be mistakenly believed to be 'background strain' caused by regional deformation alone.

Consider, for example, the following scenario: a pluton expands during intense non-coaxial deformation. The pluton is unroofed by erosion, so that a horizontal erosional surface exposes a constrictional ring at the top of the pluton, but does not expose the pluton itself. In this case, modeling shows that the geometry of exposed strains and structures is consistent with tectonic deformation alone. The exposed ring contains highly constrictional strains, therefore, foliations are poorly developed, and mineral stretching lineations are well developed, horizontal, and parallel to each other. These patterns are not uniquely diagnostic of pluton presence. In addition, because the pluton was elongated by tectonism, foliation and lineation form an extremely elongate pattern (long-upside-down-canoe shape) that is almost indistinguishable from the regional structural fabric. These foliation and lineation patterns were produced by the three-dimensional interaction between pluton-related and tectonic-related strain fields. However, because the pluton itself is not visible, the 'logical' but wrong interpretation would be that these structures were unrelated to pluton emplacement. This example shows that pluton-related control of structures observed in orogenic belts may have been overlooked in the past and, consequently, be more pervasive than previously thought.

Origin and extent of country rock deformation

To accurately evaluate pluton-related control of strains and structures in orogenic belts, it is necessary to determine how far away strains due to pluton emplacement affect the country rock. This determination is difficult because, with increasing distance from the pluton, physical and methodological limitations increase and prevent accurate measurements of subtle pluton-related strain gradients. For example: pluton-related strains become disturbed by strain fields produced by neighboring plutons that are presently exposed, buried or eroded away. In addition, with increasing distance from the pluton, strain intensities become too small and impossible to measure accurately. These stains are small but important because they may affect a country rock volume larger than the pluton itself.

Whereas pluton-related strains and structures far from plutons are difficult to measure, strains and structures closer to the pluton are not. Foliation triple points, which are map-view representations of three-dimensional strain rings, are relatively easy to determine. Modeled patterns show that the distance from ring to pluton constrains how far from the pluton intrusion-related strains may affect the country rock. For a ring to form, pluton-related strains must necessarily affect at least the region between ring and pluton and part of the country rock beyond the ring. In addition, depending on pluton-related and tectonic-related strain gradients, pluton-related strains may affect country rock well beyond the ring. For example, the pluton-related flattening region extends two body radii from the pluton (red area in Fig. 1c). The tight geometric link between ring and region affected by pluton-related strains is (1) true for both coaxial and non-coaxial deformation (Guglielmo in press a), and (2) independent of whether the pluton is pre-, syn- or post-tectonic. Therefore, the distance between the foliation triple point and the pluton helps us evaluate how far pluton-related strains affect strains in the natural country rock. For example: foliation triple points are found as far as 4 km, or 1/2 body radii, away from post-tectonic natural plutons (Fig. 5a) (Guglielmo 1993, in press b).

Guidelines for field mapping

Displacement fields caused by non-expanding rising plutons, or by non-expanding pre-tectonic plutons are

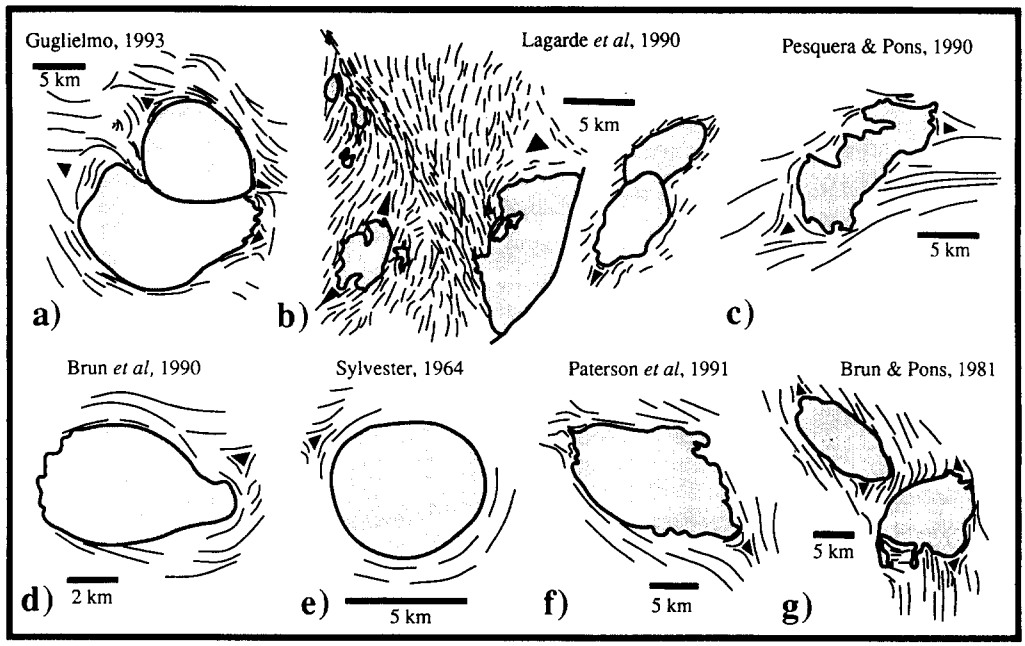

Fig. 5. Foliation patterns (black lines) around natural plutons (gray). In these examples, foliation triple points (black triangles) are probably the result of interference between pluton-related strains and regional strains. Some workers reported strains on the sides of the pluton (a, b, c, d, f & g), and some also measured strains at triple points (a, b & g). They consistently reported flattening on the sides of the pluton and constriction at foliation triple points.

expected to share a few similarities with displacement fields produced by expanding plutons. Country rocks around the upper hemisphere of a non-expanding rising pluton may show general flattening strain ellipsoids oriented radially around the pluton and strain intensities that decrease away from the pluton (Cruden 1988, 1990, Schmeling *et al.* 1988). In addition, non-expanding pretectonic plutons can alter strain fields produced in the country rock during subsequent regional deformation. Consequently, this alteration may produce foliation triple points and flattening strains that decrease away from the pluton (e.g. Paterson & Tobisch 1988). Consequently, non-expanding plutons could produce constrictional rings whose geometry approximately resembles the rings modeled herein. Therefore, although rings provide field evidence consistent with pluton expansion, they, by themselves, do not prove pluton expansion. Field relationships should be used to decide to what extent expansion occurred in the field (e.g. Ramsay 1989). In addition, radiometric ages, strain, microstructural and structural field analysis should attempt to determine: (1) timing relationships between pluton emplacement and tectonic deformation (e.g. Paterson & Tobisch 1988 and references therein); and (2) strain pattern distortions due to country rock anisotropies and neighboring plutons. Subsequently, modeled strain patterns should be adapted accordingly.

The modeled patterns provide a theoretical framework and a practical guide for the field geologist. They suggest that the ends and sides of the pluton are structural domains having distinct kinematic histories during pluton emplacement, producing structures that should be plotted and analyzed separately. The model facilitates mapping, plotting and analysis by suggesting: (1) the location, shape and structural evolution of these two domains; and (2) which aspect of the strain ellipsoid (intensity, shape or orientation) gives most information about kinematics in the country rocks.

Whenever possible, the four modeled parameters (strain intensity, shape and orientations of foliation, and lineation) should be determined for each outcrop in these two domains. The analysis of these four parameters taken together for each outcrop produces insights that are more valuable than the insights produced by each parameter taken separately. For example: low strains at the ends of a pluton are not, by themselves, a diagnostic feature. However, the combination of low strains + constriction + vertical stretching lineations + vertical foliations is kinematically more significant. In addition, the map *pattern* of each parameter is more revealing than individual outcrop measurements of the parameter. Finally, this integrated analysis is even more powerful if modeled patterns can be supplemented by incremental strain measurements (Ramsay & Huber 1983) and microstructural relationships in the country rock (Bell & Rubenach 1983, Passchier & Simpson 1986, Vernon 1989).

Additional two-dimensional patterns can be visualized by mentally rotating the three-dimensional models and erosional planes presented herein. Comparisons between these two-dimensional patterns with field-map patterns should help us understand better the kinematics around plutons in orogenic belts.

SUMMARY

The models presented in this paper simulate in three dimensions the position, type and kinematic evolution

of structures around expanding plutons in a non-coaxial tectonic environment. The simulations suggest that concave lenses of high strain magnitudes form on the sides of the pluton, whereas ellipsoidal zones of low strain magnitude form at the ends (e.g. Fig. 1i). In addition, foliation, stretching lineations and constrictional regions form irregular three-dimensional rings around the pluton (e.g. Figs. 2a and 3a).

Higher total tectonic-related strains and strain rates favor a pattern of well-defined low-strain zones, small constrictional regions, and rings that migrate towards the pluton. Conversely, higher total expansion-related strains and strain rates favor high strains uniformly distributed around the pluton, large constrictional regions and ring migration away from the pluton. Ring migration rates are much slower than tectonic deformation rates or expansion rates. The direction of ring migration controls the volume affected by strain ellipsoid interference trails, and whether flattening strains will be superposed upon constrictional strains or vice versa. Furthermore, the models suggest that strain ring existence is more dependent on total strains than on the sequence in which the strains are accumulated. In addition, strain rings may persist during pre-, syn- and post-tectonic progressive deformation, and have good chances of being preserved (e.g. as foliation triple points in map view).

Three-dimensional modeling helps us interpret map-view patterns of strain shape, strain intensity, foliations and stretching lineations around plutons. These patterns can aid in constraining shear zone orientation and sense of movement.

Finally, the modeled patterns suggest that pluton-related structures in orogenic belts can be easily mistaken for tectonic structures; consequently, erosionally unroofed plutons can be overlooked. The simulations also suggest that plutons contribute more than previously believed to deformation of the country rocks. For example, comparison between field and modeled strain patterns shows that pluton-related strains and structures may appear in country rocks beyond at least half a body radius away from the pluton.

Acknowledgements—This work was supported by National Science Foundation grant number EAR-8904706 and by a University of California President's Fellowship. I would like to thank Karen McNally and Jane Wilhelms for the use of their computers at UCSC, as well as O. Tobisch, M. P. A. Jackson and J.-P. Brun for reviewing the manuscript.

REFERENCES

Bell, T. H. & Rubenach, M. J. 1983. Sequential porphyroblast growth and crenulation cleavage developed during progressive deformation. *Tectonophysics* **92**, 171–194.

Berthé, D., Choukroune, P. & Jegouzo, P. 1979. Orthogneiss, mylonites and non-coaxial deformation of granites: the example of the South Armorican shear zone. *J. Struct. Geol.* **1**, 31–43.

Brun, J.-P., Gapais, D. & Le Theoff, B. 1981. The mantled gneiss domes of Kuopio (Finland): interfering diapirs. *Tectonophysics* **74**, 283–304.

Brun, J.-P. & Pons, J. 1981. Strain patterns of pluton emplacement in a crust undergoing non-coaxial deformation, Sierra Morena, Southern Spain. *J. Struct. Geol.* **3**, 219–230.

Brun, J.-P. 1983. Isotropic points and lines in strain fields. *J. Struct. Geol.* **5**, 321–327.

Castro, A. 1986. Structural pattern and ascent model in the Central Extramadura batholith, Hercynian belt, Spain. *J. Struct. Geol.* **8**, 633–645.

Cruden, A. R. 1988. Deformation around a rising diapir modeled by creeping flow past a sphere. *Tectonics* **7**, 1091–1101.

Cruden, A. R. 1990. Flow and fabric development during the diapiric rise of magma. *J. Geol.* **98**, 681–698.

Dixon, J. M. 1975. Finite strain and progressive deformation in models of diapiric structures. *Tectonophysics* **28**, 89–124.

Gapais, D. 1989. Shear structures within deformed granites: mechanical and thermal indicators. *Geology* **17**, 1144–1147.

Guglielmo, G., Jr. 1990. The geometry of pluton emplacement in a crust undergoing uniaxial shortening. *Geol. Soc. Am. Abs. w. Prog.* **22**, 183.

Guglielmo, G., Jr. 1992. 3-D computer graphics in modeling pluton emplacement. In: *Computer Graphics in Geology* (edited by Pflug, R. & Harbaugh, J. W.). *Lecture Notes in Earth Sciences, Volume* 41. Springer, New York, 171–185.

Guglielmo, G., Jr. 1993. Magmatic strains and constrictional points of the Merrimac pluton, northern Sierra Nevada, California: implications for timing of subduction and modeling of pluton emplacement. *J. Struct. Geol.* **15**, 177–189.

Guglielmo, G., Jr. In press a. Interference between pluton expansion and coaxial tectonic deformation: three-dimensional computer model and field implications. *J. Struct. Geol.*

Guglielmo, G., Jr. In press b. Nested plutons as geopetal structures: The Merrimac plutons, northern Sierra Nevada, California. *Geol. J.*

Guineberteau, G., Bouchez, J. L. & Vigneresse, J. L. 1987. The Mortagne granite pluton (France) emplaced by pull-apart along a shear zone: structural and gravimetric arguments and regional implications. *Bull. geol. Soc. Am.* **99**, 763–770.

Holder, M. T. 1981. Some aspects of intrusion by ballooning: the Ardara pluton. *J. Struct. Geol.* **3**, 89–95.

Howard, J. C. 1971. Computer simulation models of salt domes. *Bull. Am. Ass. Petrol. Geol.* **55**, 495–513.

Howard, M. T. 1968. Monte Carlo simulation model for piercement of salt domes. *Kansas geol. Surv. Comp. Contr.* **22**, 22–34.

Hutton, D. H. W. 1981. The main Donegal granite: lateral wedging in a syn-magmatic shear zone. *Diapirism and Gravity Tectonics: Report of a Tectonic Studies Group* (edited by Coward, M. P.). *J. Struct. Geol.* **3**, 89–95.

Hutton, D. H. W. 1982. A tectonic model for the emplacement of the main Donegal granite, NW Ireland. *J. geol. Soc. Lond.* **139**, 615–631.

Hutton, D. H. W. 1988. Granite emplacement mechanisms and tectonic controls: inferences from deformation studies. *Trans. R. Soc. Edinb. Earth Sci.* **79**, 245–255.

Jackson, M. P. A. & Talbot, C. J. 1989. Anatomy of mushroom-shaped diapirs. *J. Struct. Geol.* **11**, 211–230.

Jaeger, J. C. & Cook, N. G. 1969. *Fundamentals of Rock Mechanics*. Chapman & Hall, London.

Kerrich, R., Allison, I., Barnett, R. L., Moss, S. & Starkey, J. 1980. Microstructural and chemical transformation of granite in a shear zone at Mieville, Switzerland; with implications for stress corrosion cracking and superplastic flow. *Contr. Miner. Petrol.* **73**, 221–242.

Lagarde, J. L. & Choukroune, P. 1982. Cisaillement ductile et granitoides syntectoniques: l'exemple du massif hercynien des Jebilets. *Bull. Soc. géol. Fr.* **7**, 299–307.

Lagarde, J. L., Omar, S. A. & Rodaz, B. 1990. Structural characteristics of granitic plutons emplaced during weak regional deformation: examples from late Carboniferous plutons, Morocco. *J. Struct. Geol.* **12**, 805–821.

Lode, W. 1926. Versuche uber den Einfluss der mittleren Hauptspannung auf das fliessen des Matalle Eisen, Kupfer, and Nickel. *Z. Phys.* **36**, 913–939.

Mandal, N. & Chakraborty, C. 1990. Strain fields and foliation trajectories around pre-, syn-, and post-tectonic plutons in coaxially deformed terranes. *Geol. J.* **25**, 19–23.

Morgan, J. 1980. Deformation due to the distension of cylindrical igneous contacts: a kinematic model. *Tectonophysics* **66**, 167–178.

Nadai, A. 1963. *Theory of Flow and Fracture of Solids*. Engineering Societies Monographs. McGraw-Hill, New York.

Nicolas, A., Bouchez, J. L., Blaise, J. & Poirier, J. P. 1977. Geological

aspects of deformation in continental shear zones. *Tectonophysics* **42**, 55–73.
O'Brien, J. J. 1987. Modelling of the deformation and faulting of formations overlying an uprising salt dome. In: *Dynamical Geology of Salt and Related Structures* (edited by Lerche, I. & O'Brien, J. J.). Academic Press, London, 419–455.
Passchier, C. W. & Simpson, C. 1986. Porphyroblast systems as kinematic indicators. *J. Struct. Geol.* **8**, 831–843.
Paterson, S. R. & Tobisch, O. T. 1988. Using pluton ages to date regional deformation: Problems with present criteria. *Geology* **16**, 1108–1111.
Paterson, S. R., Tobisch, O. T. & Vernon, R. H. 1991. Emplacement and deformation of granitoids during volcanic arc construction in the Foothills terrane, central Sierra Nevada, California. *Tectonophysics* **191**, 89–110.
Pesquera, A. & Pons, J. 1990. Le pluton hercynien de Aya (Pyrénées basques espagnoles). Structure, mise en place et incidences tectoniques régionales. *Bull. Soc. géol. Fr.* **8**, 13–21.
Ramberg, H. 1967. *Gravity, Deformation and the Earth's Crust as Studied by Centrifuge Models*. Academic Press, London.
Ramberg, H. 1970. Model studies in relation to intrusion of plutonic bodies. In: *Mechanism of Igneous Intrusion* (edited by Newall, G. & Rast, N.). Gallery Press, Liverpool, 261–286.
Ramberg, H. & Sjöström, H. 1973. Experimental geodynamical models relating to continental drift and orogenesis. *Tectonophysics* **19**, 105–132.
Ramberg, H. 1974. Superposition of homogenous strain and progressive deformation in rocks. *Bull. geol. Instn. Univ. Uppsala* **6**, 35–67.
Ramsay, J. G. 1967. *Folding and Fracturing of Rocks*. McGraw-Hill, New York.
Ramsay, J. G. 1989. Emplacement kinematics of a granite diapir: the Chindamora batholith, Zimbabwe. *J. Struct. Geol.* **11**, 191–209.
Ramsay, J. G. & Huber, M. I. 1983. *The Techniques of Modern Structural Geology, Volume* 1: *Strain Analysis*. Academic Press, London.
Sacks, P. E. & Horton, J. W., Jr 1991. Riedel shear emplacement of granitic sheets at midcrustal levels of a strike slip fault: Hollister fault zone, eastern Appalachian Piedmont. *Geol. Soc. Am. Abs. w. Prog.* **23**, 175.
Sanderson, D. J. & Meneilly, A. W. 1981. Analysis of three-dimensional strain modified uniform distributions: andalusite fabrics from a granite aureole. *J. Struct. Geol.* **3**, 109–116.
Schmeling, H., Cruden, A. R. & Marquart, G. 1988. Finite deformation in and around a fluid sphere moving through a viscous medium: implications for diapiric ascent. *Tectonophysics* **149**, 17–34.
Schwerdtner, W. M. & Troeng, B. 1978. Strain distribution within arcuate diapiric ridges of silicone putty. *Tectonophysics* **50**, 13–28.
Sorgenfrei, T. 1971. On the granite problem and the similarity of salt and granite structures. *Geol. För. Stockh. Förh.* **93**, 371–435.
Soula, J. C. 1982. Characteristics and mode of emplacement of gneiss domes and plutonic domes in central-eastern Pyrenees. *J. Struct. Geol.* **4**, 313–342.
Sylvester, A. G. 1964. The Precambrian rocks of the Telemark area in south central norway. III—Geology of the Vrådal granite. *Norsk geol. Tidsskr.* **44**, 445–482.
Talbot, C. J. 1974. Fold nappes as asymmetric mantled gneiss domes and ensialic orogeny. *Tectonophysics* **24**, 259–276.
Talbot, C. J. & Jackson, M. P. A. 1987. Internal kinematics of salt diapirs. *Bull. Am. Ass. Petrol. Geol.* **71**, 1068–1093.
Tikoff, B. & Teyssier, C. 1991. Dextral shearing in the east-central Sierra Nevada magmatic arc: Implications for Late Cretaceous tectonics and passive emplacement of granite. *Geol. Soc. Am. Abs. w. Prog.* **23**, 176.
Vernon, R. H. 1989. Porphyroblast–matrix microstructural relationships—recent approaches and problems. In: *The Evolution of Metamorphic Belts* (edited by Daly, S. J. & Brown, M.). *Spec. Publs geol. Soc. Lond.* **43**, 83–102.
Woïdt, W. D. 1978. Finite element calculations applied to salt dome analysis. *Tectonophysics* **50**, 369–386.

APPENDIX

The radial expansion strain tensor is obtained from the following equations that describe the final position of a point displaced by a radial vector (Fig. A1):

$$x' = x + \Delta x \tag{A1}$$

$$\Delta x = \overline{xz'} \cos\beta \tag{A2}$$

$$\overline{xz'} = |E| \cos\alpha \tag{A3}$$

$$\cos\alpha = \frac{\overline{xz}}{d} \tag{A4}$$

$$\cos\beta = \frac{x}{\overline{xz}}, \tag{A5}$$

where d is the radius of the pluton, and $|E|$ is the magnitude of the radial displacement vector given by

$$|E| = \frac{G}{d}, \tag{A6}$$

G is an expansion parameter (Brun & Pons 1981, simplified from Jaeger & Cook 1969). The displacement field generated by the displacement vector E creates concentric flattening strains, which have strain magnitudes that decrease gradually away from the pluton. This property allows the simulation of strain patterns similar to patterns measured around natural plutons (Guglielmo 1993).

Replacing equations (A3) in (A2) and (A2) in (A1) gives the x component of the final position of the displaced point in the country rock

$$x' = x + |E| \cos\alpha \cos\beta. \tag{A7}$$

Replacing (A4), (A5) and (A6) in equation (A7) gives

$$x' = x\left(1 + \frac{G}{d^2}\right). \tag{A8}$$

Pluton expansion is assumed to be of equal magnitude in all directions, therefore displacements along the x axis are equal to displacements along the y and z axes. Consequently, the three-dimensional expansion strain tensor is given by

$$M = \begin{vmatrix} B & 0 & 0 \\ 0 & B & 0 \\ 0 & 0 & B \end{vmatrix}, \tag{A9}$$

where

$$B = 1 + \frac{G}{d^2}. \tag{A10}$$

The tensor for homogeneous simple shear (Ramsay 1967, p. 83) is given by

$$S = \begin{vmatrix} 1 & 0 & s \\ 0 & 1 & 0 \\ 0 & 0 & 1 \end{vmatrix}, \tag{A11}$$

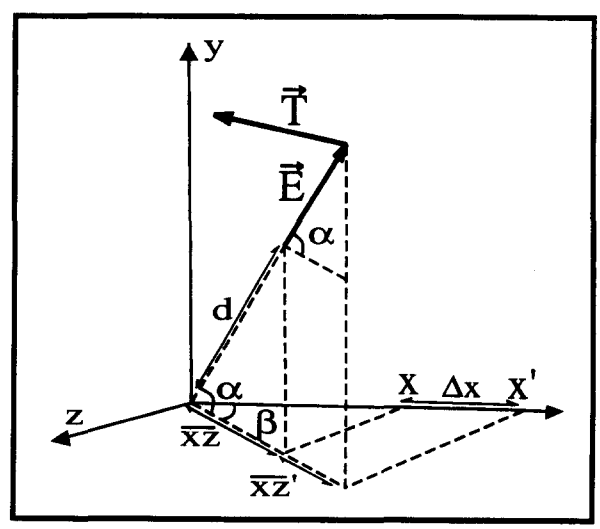

Fig. A1. Displacement vectors of expansion (**E**) and tectonic deformation (**T**).

where s is the simple shear parameter. Finally, the tensor for syntectonic expansion is given $S \times M$, that is

$$\begin{vmatrix} B & 0 & Bs \\ 0 & B & 0 \\ 0 & 0 & B \end{vmatrix}. \tag{A12}$$

Strain tensors (A9), (A11) and (A12) transform cubic elements of a simulation grid into irregular six-sided polyhedra that are used to calculate the finite strain. These polyhedra are approximated by prisms whose nine components (a–i) are used to derive the displacement equation (Ramsay 1967, p. 122):

$$\begin{vmatrix} x' \\ y' \\ z' \end{vmatrix} = \begin{vmatrix} abc \\ def \\ ghi \end{vmatrix} \begin{vmatrix} x \\ y \\ z \end{vmatrix}. \tag{A13}$$

To obtain the equation of the finite strain ellipsoid, we must solve equation (A13) in terms of x, y and z and substitute the results in the equation of a sphere (Ramberg 1974). Replacing the square matrix in equation (A13) by its inverse (D) produces

$$\begin{vmatrix} x \\ y \\ z \end{vmatrix} = D \begin{vmatrix} x' \\ y' \\ z' \end{vmatrix}. \tag{A14}$$

The equation of a sphere is given by

$$x^2 + y^2 + z^2 = 1. \tag{A15}$$

Replacing x, y and z in equation (A15) by their values from equation (A14) produces the equation of the strain ellipsoid:

$$|x'y'z'| \begin{vmatrix} (D_{11}^2+D_{21}^2+D_{31}^2) & (D_{11}D_{12}+D_{21}D_{22}+D_{31}D_{32}) & (D_{11}D_{13}+D_{21}D_{23}+D_{31}D_{33}) \\ (D_{11}D_{12}+D_{21}D_{22}+D_{31}D_{32}) & (D_{12}^2+D_{22}^2+D_{32}^2) & (D_{12}D_{13}+D_{22}D_{23}+D_{32}D_{33}) \\ (D_{11}D_{13}+D_{21}D_{23}+D_{31}D_{33}) & (D_{12}D_{13}+D_{22}D_{23}+D_{32}D_{33}) & (D_{13}^2+D_{23}^2+D_{33}^2) \end{vmatrix} \begin{vmatrix} x' \\ y' \\ z' \end{vmatrix} = 1. \tag{A16}$$

Lengths of the ellipsoid axes are given by

$$e_1 = \frac{1}{\sqrt{\lambda_1}}; \quad e_2 = \frac{1}{\sqrt{\lambda_2}}; \quad \text{and} \quad e_3 = \frac{1}{\sqrt{\lambda_3}}, \tag{A17}$$

where λ_1, λ_2 and λ_3 are the eigenvalues of the square matrix in equation (A16). The eigenvectors corresponding to these eigenvalues give the orientations of the axes of the strain ellipsoid.